

Dielectric anisotropy in the integration of Cu–SiLK™ system

Hai-Sin Tseng^a, Bi-Shiou Chiou^{a,b,*}, Wen-Fa Wu^b, Chia-Cheng Ho^a

^a Department of Electronics Engineering and Institute of Electronics, National Chiao Tung University, Hsinchu, Taiwan

^b National Nano Device Laboratories, Hsinchu, Taiwan

Received 1 December 2006; received in revised form 27 February 2007; accepted 18 April 2007

Available online 13 May 2007

Abstract

As device density and performance continue to improve, low dielectric constant (k) materials are needed for interlevel dielectric (ILD) applications. The dielectric anisotropy of polymers with low k is an important property to consider for developing ILD. This is on-going research on the integration aspects of Cu–SiLK™ system. In this study, the dielectric anisotropy of SiLK polymer was evaluated with two test structures: the metal–insulator–metal (MIM) parallel capacitor structure for the out-of-phase dielectric constant (k_{\perp}) and comb-and-serpentine interdigitated structure for the in-plane dielectric constant (k_{\parallel}). A k_{\perp} of 2.65, a k_{\parallel} of 2.75, and a dielectric anisotropy of 3.77% were obtained for SiLK. However, SiLK exhibits larger leakage current as compared to amorphous SiO₂ films. The reliability issue on the integration of Cu–SiLK is discussed.

© 2007 Elsevier B.V. All rights reserved.

Keywords: Dielectric anisotropy; Cu; SiLK; Cu-low k integration

1. Introduction

As interconnect feature size decreases and clock frequency increases, interconnect RC time delay and current density increment become the major limitations on achieving high circuit speeds and reliability. Small capacitance (C) between interconnects is required to reduce the crosstalk, insertion loss, and RC delay associated with the metal interconnect system. Therefore, the interconnect with low dielectric constant (k) material are required. Polymers, with low processing temperatures, ease of application, and good surface planarization, have attracted much attention in the application for low dielectric constant materials. However, polymer thin films are anisotropic due to the preferred chain orientation in the film plane and a ~21% difference between the in-plane dielectric constant and the out-of-plane dielectric constant was reported for a fluorinated

polyimide (DuPont EPI-136M) [1,2]. Hence, the dielectric anisotropy of low dielectric constant polymers is an important parameter in selecting low dielectric constant materials. Besides, the integration of low dielectric constant materials is a critical parameter in controlling electrical performance because it affects the propagation delay, crosstalk, and power dissipation of the integrated circuits [3–8].

This is on-going research on the integration aspects of Copper–SiLK systems. SiLK (trademark of the Dow Chemical Company) is a low-molecular-weight aromatic thermosetting polymer. SiLK films are one of the most attractive interlayer dielectrics because of their good surface planarization characteristics, low dielectric constant and high toughness [9,10]. In the previous work [11], the thermal characteristics of SiLK are investigated to evaluate the feasibility of SiLK for low dielectric constant materials. Besides, the electromigration in Cu with SiLK passivation was studied and the mechanism is explored [5,11]. In this study, the dielectric anisotropy of SiLK is investigated. In the application of low dielectric constant polymer, it is advantageous in process integration to employ an inorganic

* Corresponding author. Address: Department of Electronics Engineering and Institute of Electronics, National Chiao Tung University, Hsinchu, Taiwan.

E-mail address: bschiou@mail.edu.tw (B.-S. Chiou).

liner such as SiO₂ or Si₃N₄. The introduction of liner helps in obtaining interconnect patterns with better resolution, enhancing the dielectric breakdown strength, etc. [12]. However, the liner may behave as a current leakage path. In this work, the leakage currents between SiLK and inorganic liner SiO₂ are studied, and the pros and cons of using SiLK as low dielectric constant materials are discussed.

2. Experimental procedures

Four-inch diameter p-type (100) Si wafers with nominal resistivity of 1–10 Ω cm were used as substrates. Metal–insulator–metal (MIM) parallel-plate capacitors were prepared to measure the out-of-plane dielectric constant. A 30 nm Ta barrier layer and a 600 nm Cu film were sputtered sequentially onto the substrate to serve as the bottom electrode. SiLK films were then spin-coated, baked, and cured (90 s at 150 °C followed by 60 s at 325 °C followed by 30 min at 400 °C) to a thickness of ~650 nm. Aluminum films were then deposited as the top electrode. The out-of-plane dielectric constant (k_{\perp}) was calculated using the following equation:

$$k_{\perp} = Cd/\epsilon_0A, \tag{1}$$

where d is the thickness of the dielectric film, C is the measured capacitance, ϵ_0 is the permittivity of free space, and A is the area of the electrode. The amorphous SiO₂ films, deposited by the decomposition of tetraethyl orthosilicate, with 500 nm in thickness were deposited onto Cu electrode with PECVD (Multi-chamber PECVD, STS-MULTI-PLEX CLUSTER SYSTEM, England) at 250 °C and 100 mTorr. The dielectric constant of amorphous SiO₂ film was also measured with an MIM structure.

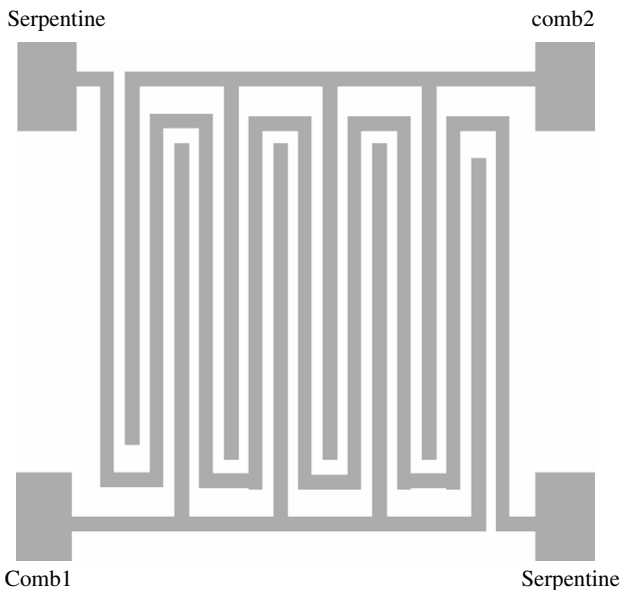


Fig. 1. Comb and serpentine interdigitated test structure for evaluating in-plane dielectric constant and interface leakage current.

For the evaluation of in-plane dielectric constant (k_{\parallel}) and interface leakage current, an interdigitated comb and serpentine structure is employed, as shown in Fig. 1. Fig. 2 gives the flow chart for the preparation of specimens. A 500 nm SiO₂ films were grown on the Si substrate. Conventional photolithography was used to obtain SiO₂ trenches (300 nm in depth) with the interdigitated pattern shown in Fig. 1. Ta (~30 nm) and Cu (~600 nm) films were then sputtered sequentially to fill oxide trenches and were annealed at 450 °C for 60 min in vacuum. Chemical

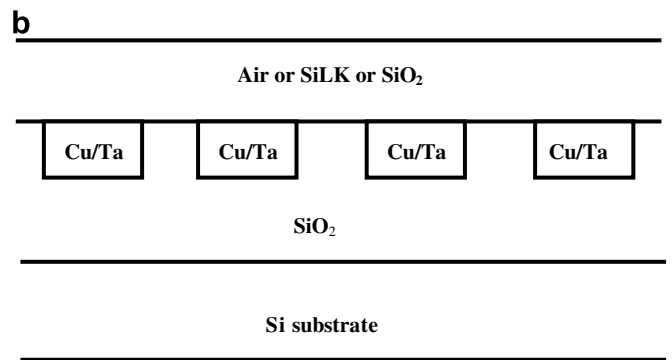
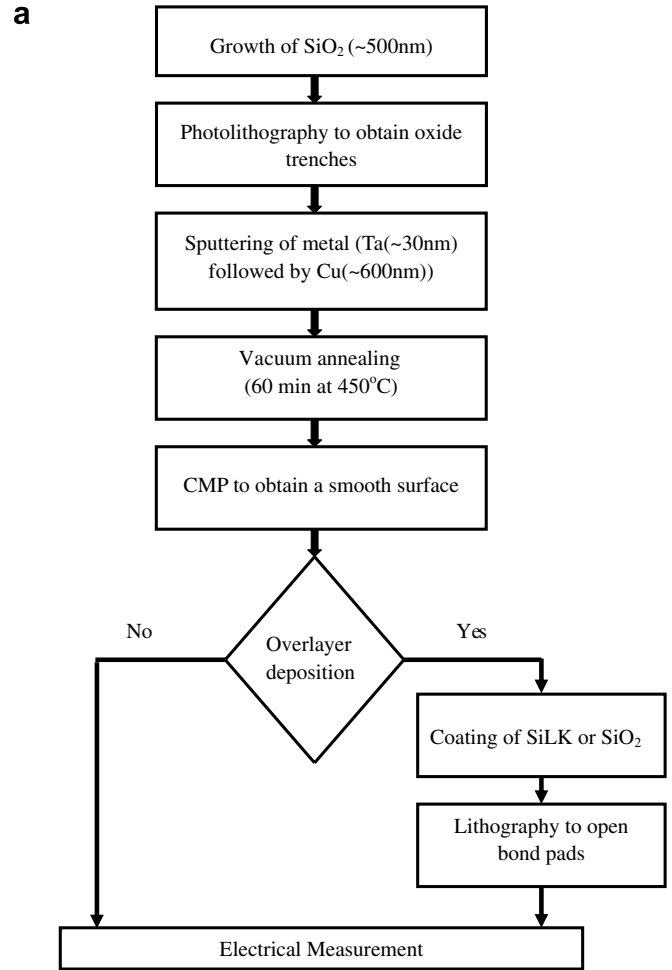


Fig. 2. (a) Flow chart for the preparation of samples and (b) schematic diagram of the sample cross-section.

mechanical polishing was then employed to obtain a smooth specimen with cross-section shown schematically in Fig. 2b. Some specimens were then coated with SiLK or SiO₂. The thickness of the coating is ~650 nm. An additional photolithography was used to open bond pads for electrical testing. A C - V analyzer (model 590, Keithley, USA) and a semiconductor parameter analyzer (HP4155B, Hewlett-Packard Co., USA) were employed to measure the capacitance and the leakage current, respectively.

3. Results and discussion

As described in Section 2, the out-of-plane dielectric constant (k_{\perp}) is measured with an MIM parallel-plate capacitor structure. The k_{\perp} of SiLK and SiO₂ is 2.65 and 4.21, respectively. Interdigitated electrode structure, shown in Fig. 1, has been used to determine the in-plane dielectric constant (k_{\parallel}) [1,2]. In order to characterize the dielectric properties of SiLK in a structure of its actual use, a multilayer test structure as fabricated as shown schematically in Fig. 2a. The capacitances between the metal line passivated with air (i.e., without passivation), SiO₂, or SiLK are measured. The interdigitated metal line structure is used to amplify the capacitance between the metal lines, as shown in Fig. 2b. The length of the serpentine metal line is about 400 μm . The capacitance measured, C , includes the capacitance contributed by SiO₂ ($C_{\text{bottom}} + C_{\text{side}}$) and the dielectric passivation (C_{top}). As shown schematically in Fig. 3a, C equals to the sum of C_{top} , C_{side} and C_{bottom} , where C_{side} is the line-to-line capacitance, and C_{top} and C_{bottom} are the fringe capacitance. The capacitance of specimens passivated with air (i.e., unpassivated), SiO₂, and SiLK are 22.6 pF, 36.9 pF, and 30.2 pF, respectively. The accuracy of measurements is ± 0.1 pF. The dielectric constant of air is ~ 1 . Because SiO₂ is amorphous and without preferred orientation, the dielectric behavior of SiO₂ should be isotropic and the dielectric constant of SiO₂ is 4.21 which obtained from the MIM structure. Because ($C_{\text{bottom}} + C_{\text{side}}$) are approximately constant for the three specimens, $C_{\text{top}} = C - (C_{\text{bottom}} + C_{\text{side}})$ is proportional to the dielectric constant of the passivation. Hence, the dielectric constant of SiLK can be interpolated from the C - k curve shown in Fig. 3b. The dielectric constant k thus obtained is 2.70 from SiLK. The k_{\perp} of SiLK is 2.65. The difference between the k_{\perp} and the k obtained from C_{top} of Fig. 3a suggests that the dielectric behavior of SiLK is anisotropic. The capacitance C_{top} consists of relatively large fringe capacitance from the extension of electric fields around the metal lines. However, it is beyond the scope of this research to analyze the electric field distribution inside the dielectric layer of the capacitor C_{top} and to calculate the in-plane dielectric constant k_{\parallel} of SiLK on the basis of the gross dielectric constant k (2.70), the out-of-plane dielectric constant k_{\perp} (2.65) and the electric field. Since the gross dielectric constant k is within the range of k_{\perp} and k_{\parallel} . It is estimated that the gross dielectric constant k is

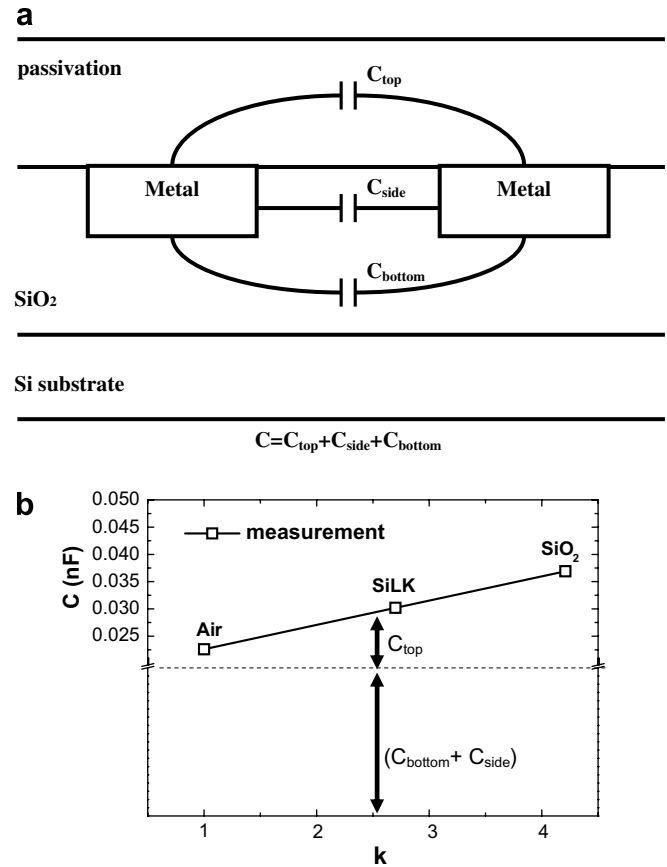
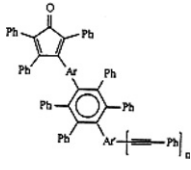
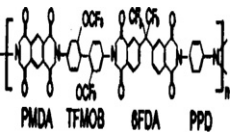
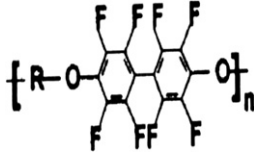
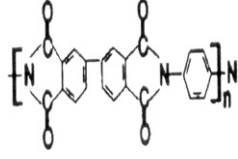


Fig. 3. (a) Schematic diagram of the capacitance between metal lines, and (b) capacitance vs. dielectric constant plot for specimens with various passivations. The measured capacitance is C , $C = C_{\text{top}} + C_{\text{side}} + C_{\text{bottom}}$, and $(C_{\text{side}} + C_{\text{bottom}})$ is constant, $C_{\text{top}} = C - (C_{\text{bottom}} + C_{\text{side}})$ is proportional to the dielectric constant of the passivation, so the dielectric constant of SiLK can be obtained by the C - k plot.

around the average of k_{\perp} and k_{\parallel} . The k_{\parallel} thus obtained is 2.75.

The dielectric anisotropy is attributed to the preferred chain orientation in the plane of the polymeric thin film, resulting in properties in the film thickness direction different from those in the film plane. Cho et al. reported that molecular structure affected the dielectric anisotropy of polymers. Rigid rod-like polymers, such as fluorinated polyimide, EPI-136M, have a strong propensity to align parallel to the substrate when solution cast due to a substrate confinement effect, while flexible chain polymers, such as fluorinated poly(aryl ethyl) (FLARE-1.51), have a smaller propensity to align parallel to the substrate and are more likely isotropic [1]. Table 1 summarizes the chemical structure and the dielectric constant of four low k polymers. Fig. 4 exhibits the percent anisotropy ($(k_{\parallel} - k_{\perp})/k_{\perp} \times 100\%$) as a function of weight and/or length of the monomer. The anisotropy data shown in Table 1 and Fig. 4 are derived from three separate studies with three different structures of multilayer test vehicles (Ref. [1,2] and this work). Polymers with low monomer weight (< 400 g/mol) exhibit small anisotropy, but no specific trend

Table 1
Chemical structure and dielectric constant of some low k polymers

Polymer	Structure	k_{\parallel}	k_{\perp}	% Anisotropy, $\Delta k = (k_{\parallel} - k_{\perp})/k_{\perp}$ (%)	Weight of monomer (i.e., $n = 1$) (g/mol)	Length of monomer (nm)	Note
SiLK		2.75	2.65	3.77	216	0.464	This work and Ref. [9]
Fluorinated polyimide (DuPont EPI-136M)		2.790	2.305	21.04	1046	0.57	Ref. [1]
Poly(aryl ethyl) (allied signal FLARE-1.51)		2.565	2.618	1.45	328	0.424	Ref. [1]
Aromatic polyimide, BPDA-PDA ^a		3.3	3.1	6.45	356	0.26	Ref. [2]

^a Poly(*p*-phenylene biphentyltetracarboximide).

is observed between the anisotropy and weight of monomer, probably due to the experimental errors and/or structural differences. However, the anisotropy increases with further increase of monomer weight, the higher the weight of monomer, the larger the dielectric anisotropy, as can be observed from Table 1 and Fig. 4. Factors that affect the evaluation of the in-plane dielectric constant and the anisotropy include measurement error (<0.5% in this study), the estimate that the gross dielectric constant is about the average of k_{\parallel} and k_{\perp} , the structure of the test vehicles, such as: aspect ratio between the electrode spacing and the dielectric thickness, the hierarchy of the various dielectric layers with respect to metallization, the dependence of the lateral capacitance on the thickness of the dielectric between metal trenches, etc.

A dielectric material reacts to an electrical field differently from a free space because it contains charge carriers that can be displaced (i.e., polarized), and charge displacements within the dielectric can neutralize a part of the applied field, and, consequently, increase the amount of charge stored. There are various possible mechanisms for polarization in a dielectric material, such as: electronic polarization, atomic polarization, molecular (orientation)

polarization, and space charge polarization. The dielectric anisotropy of the polymer is resulted from the molecular polarization which has a relaxation time corresponding to the particular material system and, in general, cannot follow the electric field when the applied frequency exceeds $\sim 10^{10}$ Hz. In this study, the applied frequency is 10^5 Hz, hence, molecular polarization contributes to the anisotropy of SiLK.

The leakage current of specimens with SiLK or SiO₂ overlayer is evaluated with the comb and serpentine interdigitated structure shown in Fig. 1. The metal lines were coated with SiLK or SiO₂ as described in the experimental procedures. Fig. 5 exhibits the comb current I_{comb} as a function of serpentine voltage V_{serp} for specimens with the different coatings. It is obvious that the leakage currents of specimens with SiLK overlayer are larger than those of specimens with SiO₂ overlayer. There are various paths for current to flow, such as: through the interface of the overlayer and the underlayer, through the bulk of overlayer, and/or through the underlayer, as shown schematically in Fig. 6a. If the majority current flows through the bulk, the leakage current should be approximately inversely proportional to the length of the path, since the

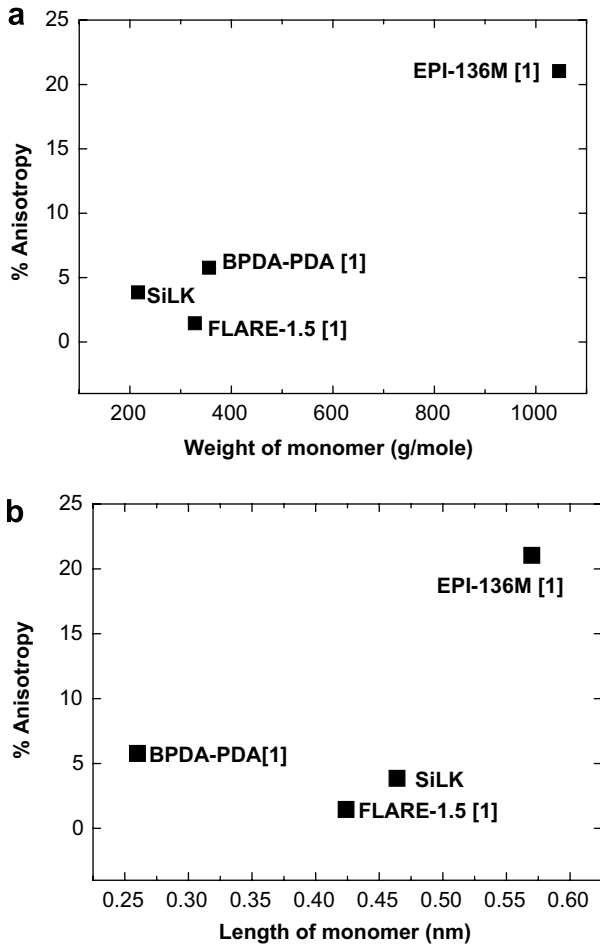


Fig. 4. Percent anisotropy ($k_{\parallel} - k_{\perp} / k_{\perp} \times 100\%$) as a function of: (a) length of monomer and (b) weight of monomer of four low k polymers.

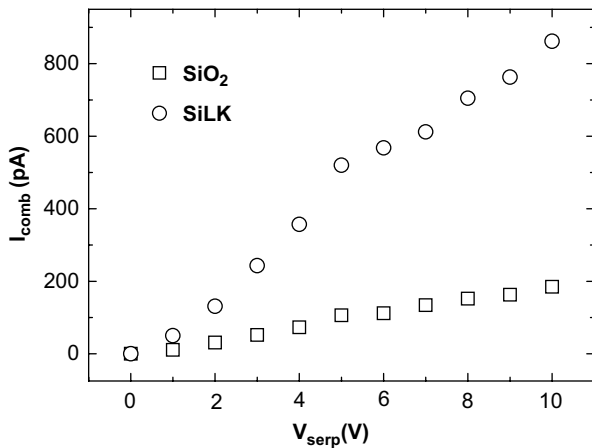


Fig. 5. I_{comb} as a function of V_{serp} for specimens coated with SiO₂ or SiLK.

resistance is proportional to the length. As shown schematically in Fig. 6b, I_{serp} should be approximately twice of I_{comb2} . However, if interface current flow dominates, then there is no apparent relation between leakage current and path length. To identify the major current leakage path,

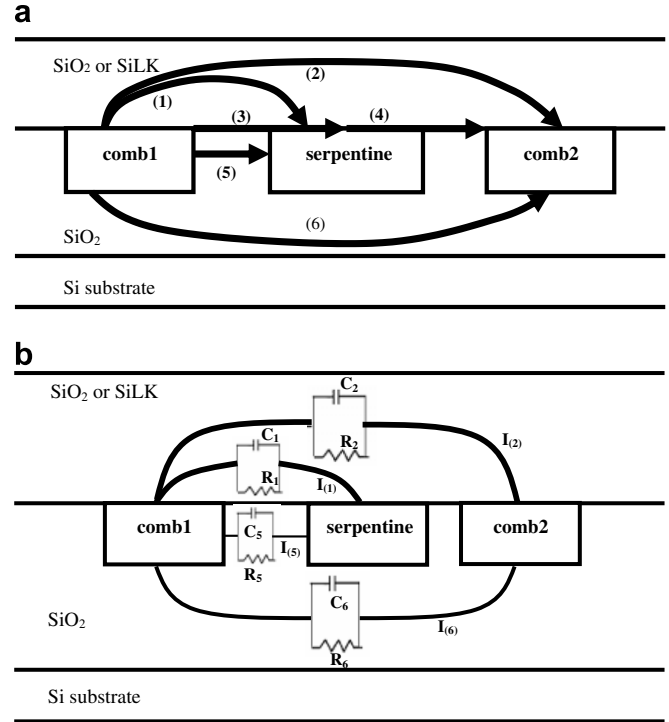


Fig. 6. (a) Partial cross-section of the specimen and possible current leakage paths indicated by arrows. Current can flow through the overlayer (1,2), the interface between the overlayer and the underlayer (3,4), and the underlayer (5,6). That is $I_{serp} = I_{(1)} + I_{(3)} + I_{(5)}$, and $I_{comb2} = I_{(2)} + I_{(4)} + I_{(6)}$. (b) Equivalent circuit model when current flow through bulk layer is the major path. That is $I_{serp} \approx I_{(1)} + I_{(5)}$, and $I_{comb2} \approx I_{(2)} + I_{(6)}$. R_i represents the resistance to current flow via path i and is proportional to the length of the path. Because the distance between comb1 and comb2 is about twice that between comb1 and serpentine, so $I_{(1)} \approx 2I_{(2)}$, $I_{(5)} \approx 2I_{(6)}$, and $I_{serp} \approx 2I_{comb2}$, if current flow through bulk is the major leakage path.

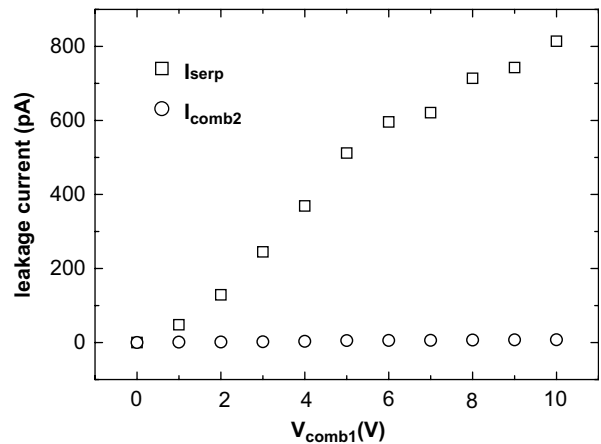


Fig. 7. Leakage current I_{serp} and I_{comb2} as a function of V_{comb1} for specimens coated with SiLK.

voltage was applied onto pad of comb1, and currents were measured at pads of comb2 and serpentine. As observed in Fig. 7, I_{serp} is much larger than I_{comb2} , and this suggests that the SiLK/SiO₂ interface is the major path for current leakage flow.

Table 2
Dielectric properties of SiLK and SiO₂ as well as reliability issues [11] for Cu–SiLK and Cu–SiO₂ system

		SiLK	SiO ₂
Dielectric constant	k_{\parallel}	2.75	4.2
	k_{\perp}	2.65	4.2
% Dielectric anisotropy	$(k_{\parallel} - k_{\perp})/k_{\perp} \times 100\%$	3.77	0
Dielectric leakage current	I_{comb} at $V_{\text{serp}} = 6 \text{ V}$ (pA) (Fig. 5)	568	112
For reliability issues [11]		Cu-passivated with SiLK	Cu-passivated with SiO ₂
Thermal impedance of Cu, °C/W		1832	1604
Electromigration (EM) lifetime of Cu	225 °C	$4.2 \times 10^5 \text{ s}$	$5.6 \times 10^5 \text{ s}$
	250 °C	$2.1 \times 10^5 \text{ s}$	$3.1 \times 10^5 \text{ s}$
interconnects at $2.8 \times 10^6 \text{ A/cm}^2$	300 °C	$2.9 \times 10^4 \text{ s}$	$5.4 \times 10^4 \text{ s}$
Activation energy Q for EM of Cu (eV)		0.71	0.89
Predicted EM lifetime ^a of Cu interconnect at $2.8 \times 10^6 \text{ A/cm}^2$	100 °C	$6.49 \times 10^7 \text{ s}$	$8.51 \times 10^8 \text{ s}$
	25 °C	$1.69 \times 10^{10} \text{ s}$	$9.04 \times 10^{11} \text{ s}$

^a The predicted EM lifetime is calculated on the Arrhenius equation: $\frac{t_{r1}}{t_{r2}} = \exp\left(\frac{Q}{kT_1} - \frac{Q}{kT_2}\right)$.

Table 2 gives a comparison between Cu–SiLKTM and Cu–SiO₂ systems. The low dielectric constant of SiLK renders it a good candidate as interlevel dielectric, however, the larger leakage current, higher thermal impedance, and the poor electromigration resistance of Cu passivated with SiLK cast the reliability concerns for Cu–SiLK system.

4. Conclusions

The dielectric anisotropy of SiLK films is studied. The out-of-plane dielectric constant (k_{\perp}), measured with an MIM structure, is 2.65. The in-plane dielectric constant (k_{\parallel}) was evaluated with a comb and serpentine interdigitated structure and an estimate to the gross dielectric constant on the basis of k_{\parallel} and k_{\perp} . The k_{\parallel} obtained is 2.75. The dielectric anisotropy of SiLK, $\sim 3.77\%$ is attributed to the molecular polarization and should fade away at high

frequencies ($>10^{10}$ Hz). The low dielectric constant renders SiLK a good candidate to replace SiO₂ for low dielectric constant material. However, Cu passivated with SiLK exhibits larger leakage current, higher thermal impedance, and shorter electromigration lifetime than that passivated with SiO₂. Hence, there is a reliability concern for the integration of Cu–SiLK system.

Acknowledgement

This work is sponsored by National Science Council, Taiwan, under the Contract Nos. NSC91-2216-E-009-023 and NSC-92-2216-E-009-007.

References

- [1] T.H. Cho, J.K. Lee, P.S. Ho, E.T. Ryan, J.G. Pellerin, J. Vac. Sci. Technol. B 18 (2000) 208–215.
- [2] A. Deutsch, M. Swaminathan, M.H. Ree, C. Surovic, G. Arjavalingam, K. Prasad, D.C. McHerron, M. McAllister, G.V. Kopsay, A.P. Giri, E. Perfecto, G.E. White, in: Proceedings, the Topical Meeting on Electrical Performance of Electronic Packaging, Monterey, California, 1993, pp. 151–154.
- [3] J.J. Senkevich, T. Karabacak, D.L. Bae, T.S. Cale, J. Vac. Sci. Technol. B 24 (2006) 534–538.
- [4] J. Liu, M. Scharnberg, J. Bao, J. Im, P.S. Ho, J. Vac. Sci. Technol. B 23 (2005) 1422–1427.
- [5] L.M. Gignac, C.K. Hu, E.G. Liniger, Microelectron. Eng. 70 (2003) 398–405.
- [6] C.C. Ho, B.S. Chiou, Microelectron. Eng. 83 (2006) 528–535.
- [7] C.C. Ho, B.S. Chiou, Microelectron. Eng. 84 (2007) 646–652.
- [8] W.L. Sung, B.S. Chiou, J. Electron. Mater. 31 (2002) 472–477.
- [9] S.J. Martin, J.P. Godschalx, M.E. Mills, E.O. Shaffer, P.H. Townsend, Adv. Mater. 23 (2000) 1769–1778.
- [10] O. Demolliens, P. Berruyer, Y. Morand, C. Tabone, A. Roman, M. Cochet, M. Assous, H. Feldis, R. Blanc, E. Tabouret, D. Louis, C. Arvet, E. Lajoinie, Y. Gobil, G. Passemard, F. Jourdan, M. Moussavi, M. Cordeau, T. Morel, T. Mourier, L. Ulmer, E. Sicurani, F. Tardif, A. Beverina, Y. Trouillet, D. Renaud, in: Proceedings, International Interconnect Technology Conference, 1999, pp. 198–199.
- [11] H.S. Tseng, B.S. Chiou, W.F. Wu, C.C. Ho, J. Electron. Mater. 33 (2004) 796–801.
- [12] J.D. Plummer, M. Deal, P.B. Griffin, Silicon VLSI Technology: Fundamentals, Practice and Modeling, Prentice Hall, 2000, p. 58.